Microstructure and Structural Defects of Bulk Amorphous $Fe_{64}Co_{10}Y_6B_{20}$ Alloy

KATARZYNA BLOCH*
Institute of Physics, Faculty of Production Engineering and Materials Technology, Czestochowa University of Technology, 19 Armii Krajowej Str., 42-200 Czestochowa, Poland

This paper presents studies relating to the structure and soft magnetic properties of the following bulk amorphous alloys $Fe_{64}Co_{10}Y_6B_{20}$. Samples were prepared by injecting the molten alloy into a water-cooled copper mould in the form of rods. On the basis of the performed X-ray diffraction studies and Mössbauer spectroscopy, it was found that investigated samples were amorphous in the as-cast state. The influence of structural defects on the magnetization process was investigated within high magnetic fields known as the area of the approach to ferromagnetic saturation.

Keywords: bulk amorphous alloy, Mossbauer spectroscopy, structural defects, Holstein-Primakoff paraprocess

The amorphous alloys are characterized by unique magnetic properties, attributed to their structure [1-11]. These alloys are obtained using much lower quenching speeds (i.e. 10^{-1}–10^{-2} K/s) than commonly-made classical amorphous alloys [12-19]. The longer production process of the amorphous alloys forces the diffusion of atoms, which is the cause of their structural relaxation. In strong magnetic fields, within the region known as the approach to the ferromagnetic saturation, the specimen does not reach the full saturation due to structural defects [20-36]. These defects are sources of short-range and middle-range stresses. As a result of magneto-elastic interaction between stress and magnetization, a non-collinear magnetic structure occurs. Magnetization (M) of an amorphous alloy in a strong magnetic field (H), according to H. Kronmüller's theory, can be described by the equation called the law of the approach to ferromagnetic saturation [37-39]:

$$\mu_0 M(H) = \mu_0 M_S \left(1 - \sum_{n=1}^{4} a_{n/2} \Big/ \mu_0 H^{n/2}\right) + \\ + \chi \mu_0 H + b(\mu_0 H)^{1/2} \quad (1)$$

where:

M_s - saturation magnetization,

$a_{n/2}$, b - coefficients,

χ - magnetic susceptibility,

μ_o - magnetic permeability of the vacuum,

$a_{n/2} / \mu_o H^{n/2}$ - the term expressing the influence of structural defects,

n=1 for point defects,

n=2 or n=4 for linear defects,

$\chi\mu_o H$ - the term resulting from paramagnetism of electron band and diamagnetism of complete atomic shells, $b(\mu_o H)^{1/2}$ expression- determining an increase in magnetization due to damping of the spin-waves by the magnetic field.

The term $a_{1/2}/(\mu_o H)^{1/2}$ in the equation (1), related to the point defects, is described as follows:

$$\frac{a_{1/2}}{(\mu_o H)^{1/2}} = \mu_0 \frac{3}{20 A_{ex}} \left(\frac{1+\nu}{1-\nu}\right)^2 G^2 \lambda_S^2 (\Delta V)^2 N \left(\frac{2A_{ex}}{\mu_0 M_S}\right)^{1/2} \frac{1}{(\mu_0 H)^{1/2}} \quad (2)$$

where:

A_{ex} - exchange constant,

ν - Poisson's ratio,

G - shear modulus,

λ_s - saturation magnetostriction,

ΔV - additional specimen volume related to point defects,

N - volume density of point defects.

If his term is dominant, the equation (1) takes the form of the first law of approach to the ferromagnetic saturation.

The terms $a_1 / \mu_o H$ and $a_2 / (\mu_o H^2)$ in equation 1 are related to the linear defects, which internal stress field is equivalent to the field generated by the linear dislocation dipoles of the D_{dip} width, the effective Burgers vector b_{eff}, and the surface density N.

If $\chi_H D_{dip} < 1$, where χ_H is the inversed exchange distance described by the equation:

$$\chi_H = \sqrt{\frac{H\mu_0 M_S}{2A_{ex}}} \quad (3)$$

the dominant role in the equation (1) plays the term $a_1 / \mu_o H$ equal to:

$$\frac{a_1}{\mu_0 H} = 1{,}1\,\mu_0 \frac{G^2\lambda_s^2}{(1-\nu)^2} \frac{Nb_{eff}}{M_S A_{ex}} D_{dip}^2 \frac{1}{\mu_0 H} \quad (4)$$

and the equation (1) takes the form of the second law of approach to the ferromagnetic saturation.

For $\chi_H D_{dip} > 1$ the term $a_2/(\mu_0 H)^2$ is dominant and can be expressed by the equation:

$$\frac{a_2}{\mu_0 H^2} = 0{,}456\,\mu_0 \frac{G^2\lambda_s^2}{(1-\nu)^2} \frac{Nb_{eff}}{M_S^2} D_{dip}^2 \frac{1}{(\mu_0 H)^2} \quad (5)$$

Then the form of the equation (4) comes down to the third law of approach to the ferromagnetic saturation.

By studying the approach to ferromagnetic saturation one can determine the type of structural defects and on that basis draw a conclusion concerning the atomic packing density in the alloy.

For high values of magnetic fields, near the magnetic saturation point, when structural defects no longer influence the magnetization process, further magnetization increase proceeds according to the term $b(\mu_0 H)^{1/2}$, describing the Holstein–Primakoff paraprocess [39-41]. This process is related to the damping of the thermally induced spin waves by the magnetic field.

* email: 23kasia1@wp.pl

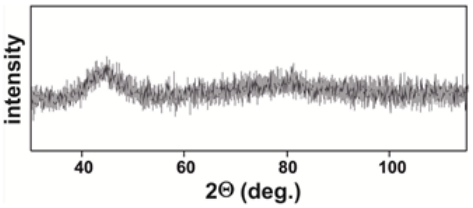

Fig. 1. X-ray patterns obtained for $Fe_{64}Co_{10}Y_6B_{20}$ alloy in the as- quenched state

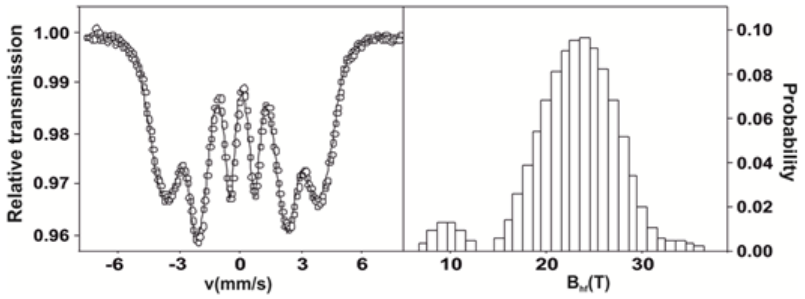

Fig. 2. Mössbauer spectra and corresponding hyperfine field induction distribution for investigated alloy

Coefficient *b* is related to the spin-wave stiffness parameter D_{sp} by the formula [42, 43]:

$$b = 3{,}54 g\mu_0\mu_B \left(\frac{1}{4\pi D_{sp}}\right)^{3/2} kT(g\mu_B)^{1/2} \qquad (6)$$

where:

g - Lande splitting factor

μ_B - Bohr magneton.

Computational details

Samples of the test alloy were obtained by injection of liquid material into a copper water-cooled mold. The obtained alloy samples were in the form of rods of 20 mm in length and 1 mm in diameter. The produced alloy samples were subjected to X-ray diffraction studies using a BRUKER diffractometer model ADVANCE 8. The camera was equipped with a cobalt X-ray lamp. The measurements were conducted within 2Θ angle ranging from 30 to 120° with a measurement step of 0.02 ° and a measurement time of 5 s.

Microstructure of alloys was investigated using POLON Mössbauer spectrometer. The γ radiation source was a cobalt 57Co isotope placed in rhodium matrix, with a activity of 50 mCi and a half-life of 270 days. The NORMOS program has been used to analyze transmission of Mössbauer spectra, which enables the distribution of experimental spectra into component spectra and to determine the distribution of induction of superfine field P(B). Distribution of induction of superfine fields on ^{57}Fe nuclei was determined according to the Hesse-Rübatsch method.

Measurement of magnetization as a function of magnetic field induction in strong magnetic fields was done using a vibration magnetometer (LAKE SHORE model 7301) in the range of 0 to 2 T. The results of magnetization studies were analyzed according to H. Kronmuller's theory. All structural, microstructure and magnetic properties investigations were performed at room temperature for low-energy crushed samples.

Results and discussions

Figure 1 shows the X-ray diffraction images of the investigated samples in the as-quenched state.

As indicated by the results of X-ray diffraction results obtained for alloy $Fe_{64}Co_{10}Y_6B_{20}$ samples had an amorphous structure. In the obtained patterns, the broad diffused maximum characteristic to amorphous material is visible. Such a diffraction pattern demonstrates the lack of translational symmetry and angular correlation in the spatial distribution of atoms.

The transmission Mossbauer spectra and corresponding hyperfine field induction distributions for investigated alloys are presented in figure 2.

Mossbauer's transmission spectra consist of wide unbalanced overlapping lines, which is typical of the spectra obtained for amorphous materials. Using the Normos software, a distribution of induction of superfine fields was obtained. In this layout we can distinguish two components, low and high one. The presence of these two components is due to the presence of different surrounding of iron atoms. The low field component is connected with areas with high concentration of iron and small distances between them. High-field component corresponds to areas where there are other atoms in the vicinity of iron atoms such yttrium and boron [43, 44].

Figure 3 shows the static magnetic hysteresis loop measured for the $Fe_{64}Co_{10}Y_6B_{20}$ alloy.

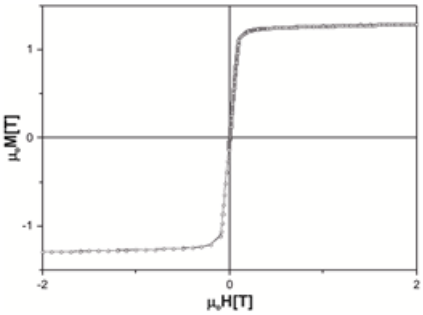

Fig. 3. Static hysteresis loop obtained for the investigated alloy in the state after solidification

Based on magnetic tests performed using a vibration magnetometer, it was found that the static hysteresis loop recorded for the studied alloy was typical of magnetic materials with so-called soft magnetic properties. According to these measurements, the saturation magnetization and the coercive field are determined respectively to M_s = 1.29 T, H_c = 24 A/m.

Figure 4 shows the primary magnetization curve measured for bulk amorphous samples.

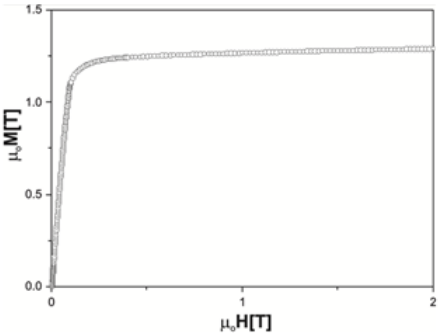

Fig. 4. Primary magnetization curve for alloy samples $Fe_{64}Co_{10}Y_6B_{20}$

By analyzing the primary magnetization curve in the area called the approach to ferromagnetic saturation, according to H. Kronmuller's theory, the type of structural defects present in the sample were determined.

Figure 5 show s the high-field magnetization curves M/Ms ($(\mu_0 H)^{-1/2}$) for the investigated alloy.

In the magnetic fields near the ferromagnetic saturation (fig. 5) the linear dependence of reduced magnetization from ($(\mu_0 H)^{-1/2}$) is visible the range of magnetizing fields from 0.29 T to 0.54 T. This means that in this magnetic field the magnetization process occurs through microscopic rotation of magnetic moments near point defects.

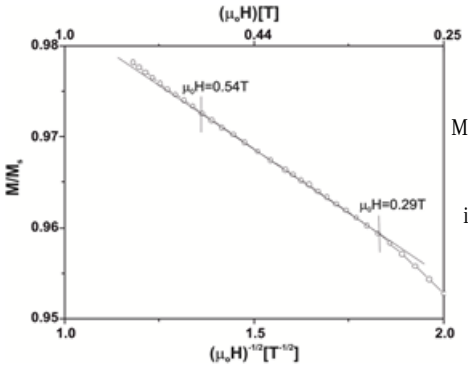

Fig. 5. Magnetization curve in function of $(\mu_0 H)^{-1/2}$ for the investigated alloy

With the increase of the intensity of the magnetizing field (> 0.66 T), there is an increase in magnetization due to the thermal stimulation of excited spin waves, the so called Holstein-Primakoff paraprocess (fig. 6).

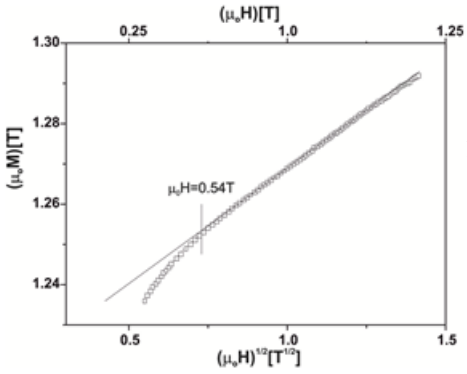

Fig. 6. Magnetization curve in function of $(\mu_0 H)^{1/2}$ for the investigated alloy

Conclusions

Using a method of injecting the alloy material into a copper mold, a massive $Fe_{64}Co_{10}Y_6B_{20}$ alloy was obtained in the form of rods of 1 mm in diameter and 20 mm in length. Based on structural and microstructure studies, the alloy in the solidified state has an amorphous structure. In addition, magnetic properties were investigated in strong magnetic fields. Magnetization curves were analyzed according to H. Kronmuler's theory. This theory provides an indirect way of studying the stresses of the structure, determining their quality and impact on the high-field magnetization process. The results of investigations presented in this paper allowed to state that magnetization process performed for the amorphous $Fe_{64}Co_{10}Y_6B_{20}$ alloy is influenced by point defects. For the examined alloy, the magnetization process in strong magnetic fields (above the range where the relationships involving the influence of structural defects are valid) proceeded as a result of Holstein–Primakoff paraprocess, i.e. by damping of the thermally induced spin waves by the magnetic field.

References

1.INOUE, A, GOOK, J. S., Mater. Trans. JIM 36, 1995, p. 1180.
2.INOUE, A., KATSUYA, A., Mater. Trans. JIM 37, 1996, p. 1332.
3.INOUE, A., ZHANG, T., ITOI, T, TAKEUCHI, A., Mater. Trans. JIM 38, 1997, p. 359.
4.INOUE, A., KOSHIBA, H., ITOI, T., MAKINO, A., Appl. Phys. Lett. 73, 1998, p. 744.
5.NABIALEK, M., Arch. Metall. Mater.61, 2016, p. 445.
6.NABIALEK, M., J. Alloys Comp. 642, 2015, p. 98.
7.GRUSZKA, K., NABIA£EK, M., BLOCH, K., OLSZEWSKI, J., Nukleonika 60, 2015, p. 23.
8.INOUE, A., Mater. Sci. Fundations 6, 1998, p 1.
9.PIETRUSIEWICZ, P., NABIAAEK, M., Acta Phys. Pol. A, 131 nr 4, 2017, p. 678.
10.PIETRUSIEWICZ, P., NABIAAEK, M., Acta Phys. Pol. A, 130 nr 4, 2016, p. 920.
11.NABIALEK, M., PIETRUSIEWICZ, P., SZOTA, M., DOŒPIAL, M., J(DRYKA, J., SZOTA, K., LESZ, S., Arch. Metall. Mater., 57 nr 1, p. 223.
12.THOMAS, T., GIBBS, M. R. J, J. Magn. Magn. Mater., 103, 1992, p. 97.
13.SOBCZYK, K., SWIERCZEK, J., GONDRO, J., ZBROSZCZYK, J., CIURZYNSKA, W., OLSZEWSKI, J., BRAGIEL, P., LUKIEWSKA, A., RZACKI, J., NABIALEK, M., J. Magn. Magn. Mater., 324, 2012, p. 540.
14.HASIAK, M., SOBCZYK, K., ZBROSZCZYK, J., CIURZYNSKA, W., OLSZEWSKI, J., NABIALEK, M., KALETA, J., SWIERCZEK, J., LUKIEWSKA, A., IEEE Trans. Magn. **11**, 2008, p. 3879.
15.BRAND, A., Nuclear Instruments and Methods in Physics Research Section B, **B28**, 1987, p. 398.
16.OLSZEWSKI J., ZBROSZCZYK J., SOBCZYK K., CIURZYNSKA W., BRyGIEL P., NABIALEK M., SWIERCZEK J.,. HASIAK M, LUKIEWSKA A., Acta. Phys. Pol. A **114**, 2008, p. 1659.
17.INOUE A., Bulk amorphous alloys with soft and hard magnetic properties**,** Materials Science and Engineering A, **A226-228**, 1997, p. 357.
18.NABIALEK M.G., DOSPIAL, M.J., SZOTA, M., PIETRUSIEWICZ, P., JEDRYKA, J., J. Alloys Comp., **509**, nr 7, 2011, p. 3382.
19.PIETRUSIEWICZ, P., NABIALEK M., DOSPIAA M., GRUSZKA K., BLOCH, K., GONDRO, J., BRGIEL, P., SZOTA, M., STRADOMSKI, Z., J. Alloys Comp., **615** nr S1, 2015, p. S67.
20.NABIALEK, M., SZOTA, M., DOSPIAL, M., PIETRUSIEWICZ, P., WALTERS, S., J. Magn. Magn. Mater., **322**, nr 21, 2010, p. 3377.
21.NABIALEK, M., DOSPIAL, M., SZOTA, M., PIETRUSIEWICZ, P., Mater. Sci. Forum, **654-656**, 2010, p. 1074.
22.NABIALEK, M., DOBRZANSKA-DANIKIEWICZ, A., PIETRUSIEWICZ, P., STRADOMSKI, Z., DOSPIAL, M., SZOTA, M.,GONDRO, J., LESZ, S., Acta Phys. Pol. A, **126**, 2014, nr 1, p. 112.
23.GONDRO, J., BLOCH, K., NABIALEK, M., GARUS, S., Materiali in tehnologije/Materials and technology **50**, 2016, p. 559.
24.SZOTA, M., Arch. Metall. Mater. **60** (4), 2015, p. 3095.
25.IONESCU, D., MATASARU, D., RADU, V., University Politehnica of Bucharest Scientific Bulletin-Series a-Applied Mathematics and Physics, **75**, no. 4, 2013, p. 265.
26.NABIALEK, M., BLOCH, K., SZOTA, M., SANDU, A.V., Mat.Plast, **54**, no. 3, 2017, p. 491.
27. BlOCH, K., NABIALEK, M., GRUSZKA, K., Rev.Chim.(Bucharest), **68**, no. 4, 2017, p. 698
28.NABIALEK, M., FUZER, J., DAKOVA, L., PIETRUSIEWICZ, P., Rev. Chim.(Bucharest), **68**,no. 5, 2017, p. 1098.
29.SANDU, A.V., CIOMAGA, A., NEMTOI, G., BEJINARIU, C., SANDU, I., Microscopy Research And Technique, **75**, no. 12, 2012, p. 1711.
30.CIMPOESU, N., STANCIU, S., VIZUREANU, P., CIMPOESU, R., ACHITEI, D.C., IONITA, I., Journal of Mining and Metallurgy Section B-Metallurgy, **50**, no. 1, 2014, p. 69.
31.VIZUREANU, P., AGOP, M., Materials Transactions, **48**, no. 11, 2007, p. 3021.
32.SANDU, A.V., CODDET, C., BEJINARIU, C., J. Optoelectron. Adv. Mater. **14**, 2012, p. 699.
33.ASANDULUI, M., LUPU, D., PETRISOR, M.B., Transformations In Business & Economics, **14**, no. 2A, 2015, p. 498.
34.PUSKAS, A., MOGA., L., CORBU., O., SZILAGYI, H., Nano, Bio And Green - Technologies For A Sustainable Future, Vol **II** (SGEM 2015), 2015, p. 203.
35.TOMA, S.L., BEJINARIU, C., GHEORGHIU, D.A., BACIU, C., Advanced Materials Research, **814**, 2013, p. 173.
36.GRUSZKA, K., NABIA£EK, M., SZOTA, M., Rev.Chim.(Bucharest), **68**,no.2, 2017, p. 408.
37.KRONMULLER, H., IEEE Trans. Magn., **15**, 1979, p. 1218.
38.KRONMULLER, H., ULNER, J., J. Magn. Magn. Mater. **6**, 1977, p. 52.
39.KRONMULLER, H., J. Appl. Phys. **52**, 1981, p. 1859.
40.HOLSTEIN, T., PRIMAKOFF, H, Phys. Rev. **58**, 1940, p. 1098.
41. BlOCH, K.. NABIA£EK, M., Acta. Phys. Pol. A **127**, 2015, p. 442.
42.KOHMOTO, O., J. Appl. Phys. **53**, 1982, p. 7486.
43.VASQUEZ, M., FERNENGEL, W., KRONMÜLLER H., Phys. Stat. Sol., **115**, 1989, p. 547
44.GONDRO, J., J. Magn. Magn. Mater. **432**, 2017, p. 501.

Manuscript received: 3.04.2017